ELSEVIER

Polymer 41 (2000) 5385–5392

polymer

Measuring the effects of dissolved oxygen in styrene emulsion polymerization

M.F. Cunningham*, K. Geramita, J.W. Ma

Department of Chemical Engineering, Queen's University, Kingston, Ontario, Canada K7L 3N6

Received 9 July 1999; received in revised form 24 September 1999; accepted 27 September 1999

Abstract

The effects of oxygen in the emulsion polymerization of styrene have been studied by varying the initial dissolved oxygen concentration in the aqueous phase. Using different initial levels of dissolved oxygen corresponding to 0, 50, 80, 90 and 100% of saturation, the induction period, conversion kinetics, molecular weight and particle size were investigated. The length of the induction period did not vary linearly with the initial oxygen level, suggesting diffusion from the headspace to the aqueous phase was an important factor. Partitioning calculations and experimental data suggest oxygen should be modeled as both a water-soluble and monomer-soluble inhibitor.

Keywords: Emulsion polymerization; Oxygen; Inhibition

1. Introduction

It has long been recognized that the presence of oxygen in emulsion polymerizations (and other free radical polymerizations) can have detrimental effects on the course of reaction, including causing inhibition periods and retarding the reaction rate [1–14]. Dissolved oxygen, one of the most common impurities in real systems, consumes radicals and can effect the radical entry rate into the particles and micelles. In an industrial emulsion polymerization, there are two reasons why oxygen is at least partially removed from the system prior to starting the reaction. First is the desire to minimize or eliminate induction periods and/or rate retardation, both which decrease reactor productivity and therefore increase process cost. Second is the safety concern of operating a reactor with potentially explosive organic monomer vapors in an oxygen-rich headspace. However in most industrial settings, it is not practical to achieve the near-zero oxygen levels that are obtained in laboratory experiments. Consequently, low levels of oxygen are present in industrial reactions. As noted by de Arbina et al. [1], inhibition and retardation are typically the cause of run to run variability.

Relatively few publications have addressed the issue of oxygen effects in emulsion polymerization. It is common to assume oxygen behaves as an ideal water-soluble inhibitor, and therefore results in an induction period that persists until all oxygen is consumed followed by a normal reaction profile. However it will be seen that this is not true. Experimental data collected in this study show that inhibition and retardation coexist, that there are effects on molecular weight and particle size, and the reaction commences while oxygen is still present.

De Arbina et al. [1] conducted a calorimetric study on the influence of oxygen in seeded styrene emulsion polymerization and the seeded emulsion copolymerization of styrene and butyl acrylate. Runs were done using different nitrogen purge flowrates, different headspace/liquid phase volume ratios, different seed diameters, particle number and initiator concentration. They observed oxygen caused an inhibition period, but also reduced the reaction rate. In a thorough review of the literature on oxygen effects, they discuss the issue of whether oxygen kinetically behaves as an 'ideal' inhibitor. There are numerous cases where apparently anomalous behavior suggests oxygen sometimes acts more like a retarder than an inhibitor. Their alternative explanation for the observed anomalies is the existence of mass transfer limitations from the reactor headspace to the latex, resulting in a gradual, continuous flow of oxygen into the liquid phase. Their own experiments showed induction time decreased with increasing initiator concentration. Also, when the headspace to liquid phase ratio was decreased, the induction period was reduced and the reaction rate increased.

Nomura et al. [9] also considered the role of headspace in

* Corresponding author. Tel.: +1-613-533-2782; fax: +1-613-533-6637.
E-mail address: cunning@chee.queensu.ca (M.F. Cunningham).

0032-3861/00/$ - see front matter
PII: S0032-3861(99)00739-9

Table 1
Formulation used in all experiments

Polymerization recipe (values in grams)	
Styrene	204.50
Water	545.50
Sodium lauryl sulfate (SLS)	2.50
Sodium bicarbonate	0.36
Potassium persulfate (KPS)	0.54

interpreting the effects of oxygen. Styrene emulsion polymerizations were run under three different atmospheres of varying, but unknown, purity (oxygen content) and at different agitation rates. Pronounced retardation was observed at high agitation speed. When a surface float was placed on top of the liquid phase, retardation did not increase at high agitation speed. Nomura attributed these results to the diffusion limited transfer of oxygen from the headspace, and recommended a policy of minimizing headspace.

The only comprehensive combined modeling and experimental work in this area was reported by Huo et al. [7] and Penlidis et al. [6] in their study of impurity effects in emulsion polymerization. Case I and Case II kinetics were considered separately. Because styrene polymerizations follow Case II kinetics, the findings of Huo et al. are most pertinent to this work. Their study examined the effects of both water-soluble and monomer-soluble impurities. They note that although oxygen is often treated as a water-soluble impurity, it is in fact also appreciably soluble in styrene. An ideal water-soluble impurity causes an induction period, followed by a normal reaction (i.e. rate, molecular weight and particle size are not affected). Huo et al. presented experimental data for styrene emulsion polymerization with added hydroquinone as the water-soluble impurity. Induction times increased as the hydroquinone concentration increased from 20 to 100 ppm.

The effects of monomer-soluble impurity (*tert*-butylcatechol) were also examined by Huo et al. Inhibitors that reside in the styrene inhibit the growth of radicals within particles and therefore reduce the reaction rate. The nucleation period may also be extended because of the reduction in the particle growth rate. Curiously, the net effect can be an increase in the overall polymerization rate once all the impurity has been consumed because of the larger particle number, as observed by Huo et al. under some conditions. Final particle size is reduced due to the larger particle number. Nomura et al. [9] reported similar findings, noting that the reaction rate following a long retardation period was often greater than after a shorter retardation period. The mathematical modeling efforts of Huo et al. demonstrated the ability of their model to predict the observed experimental behavior.

While the studies reported above have made significant contributions to understanding oxygen effects, none have actually measured dissolved oxygen concentrations in their experimental work. In this study, a dissolved oxygen meter was used to collect quantitative measurements of the dissolved oxygen concentration in the aqueous phase at the beginning and end of reaction. (The sensitivity of the probe to monomer prevented data collection throughout the run). Different initial oxygen levels were used in styrene emulsion polymerizations. Induction periods were found to vary nonlinearly with initial oxygen concentration. Conversion and molecular weight were determined at various times during the run. Thermodynamic data were used to calculate initial levels of oxygen in the styrene phase and the reactor headspace. It will be shown that oxygen cannot be treated as only a water-soluble impurity because of significant partitioning into the monomer phase. The role of headspace oxygen was also found to be significant, providing quantitative support of previously reported findings [1–9].

2. Experimental

Styrene monomer (99%), as received from Aldrich Chemical Co., was washed three times with a 10 wt% solution of sodium hydroxide, washed three times with distilled water, dried over calcium chloride and then distilled under vacuum. Sodium lauryl sulfate emulsifier (99%, SIGMA Chemicals), potassium persulfate initiator (99%, Fisher Chemicals), sodium bicarbonate buffer (Fisher Chemicals) and hydroquinone (HQ) (99%, Aldrich Chemical Co.) were all used as received. Distilled, deionized water was used throughout.

All polymerizations reactions were performed in a one liter glass reactor (10 cm diameter) with a six-bladed, 6 cm diameter, impeller mounted 3 cm above the bottom of the reactor. A Tamson Model 5 microprocessor controlled water bath was used to maintain a constant bath temperature. The reactor was equipped with a reflux condenser with a check valve, a sampling port, a thermometer and an inlet for nitrogen flow. A Mettler Toledo Model 4300 Dissolved Oxygen Microprocessor Transmitter with an Ingold Dissolved Oxygen Sensor was used to determine the oxygen levels in the emulsion. Molecular weights and molecular weight distributions were measured at 25°C in tetrahydrofuran (THF) on a Waters Gel Permeation Chromatograph (Model 2690 Alliance) equipped with Waters Styragel columns (pore sizes 500, 10^3, 10^4, 10^5 and 10^6 Å), Millenium software and a DRI detector. A calibration curve was constructed from polystyrene standards spanning a molecular weight range of $8.7 \times 10^2 - 2.8 \times 10^6$ AMU.

The variance of the measurements obtained from the dissolved oxygen meter was determined by tests performed with pure water at 100% saturation of dissolved oxygen at three temperatures (22, 40 and 60°C). Tests were repeated five times at each temperature level. Dissolved oxygen saturation levels for solutions of water/surfactant and water/surfactant/monomer (at the above-mentioned

Table 2
Measured dissolved oxygen levels at 100% saturation in various solutions

Temperature	Water (theoretical, from Henry's law constant [15])	Water (experimental)	Water and surfactant	Water, surfactant and monomer
60°C	5.37 ppm	5.40 ppm	5.58 ppm	6.53 ppm

temperatures) were also determined. Solutions contained either 0.3 wt% surfactant (sodium lauryl sulfate) or 0.3 wt% surfactant and 20 wt% monomer.

All polymerization runs were performed using the formulation outlined in Table 1. The reactor water bath was set at 60°C. Water, surfactant and buffer were added to the reactor and mixed until dissolved. Then monomer was added, the reactor vessel placed in the water bath and mixed at an agitation speed of 400 rpm to form an emulsion. Both nitrogen and air were bubbled through the mixture (alternately) until the desired dissolved oxygen level was obtained (100, 90, 80, 50 or 0% saturation). Dissolved oxygen readings were not taken continuously during reaction as the monomer chemically attacks the probe at the reaction temperature upon prolonged exposure, however the dissolved oxygen content at the completion of the run was measured. Sampling times varied with initial dissolved oxygen content, as the time between initiator addition and the commencement of polymerization was affected by the presence of dissolved oxygen. Samples were taken approximately every fifteen minutes for the first 45 min after the commencement of polymerization and then at another two to four times during the course of the polymerization. Samples (15 ml) were shortstopped with 2 ml of a 4 wt% HQ solution and placed in an ice bath. During sampling, a low nitrogen flow was introduced to in the reactor headspace (close to the sampling port) to minimize diffusion of atmospheric oxygen back into the reactor headspace. The time the sampling port was open was about five seconds. Samples were precipitated into methanol, filtered under vacuum and dried under vacuum. Conversions were determined gravimetrically. Mean particle diameter was estimated from scanning electron microscope photographs.

3. Results

The reliability of the dissolved oxygen measurement technique was established prior to conducting any polymerization experiments. Reproducibility of the oxygen measurements was excellent. Variance was determined with the pure water and water/surfactant solutions. The average variance was 1.24×10^{-3} ppm and was independent of solution temperature or composition. This corresponds to a 95% confidence interval of approximately ± 0.070 ppm for any given measurement. Dissolved oxygen levels at saturation showed little change upon the addition of surfactant (SLS) to pure water, but did increase upon addition of styrene to the water/SLS solution (Table 2). The saturation value for pure water (5.40 ppm) agrees well with the value of 5.37 ppm predicted using literature values of the Henry's Law constant [15]. A saturated water or water/SLS/styrene solution sparged with high-purity nitrogen would show a decrease in dissolved oxygen level to <0.05 ppm within 10 min.

Experiments were conducted using five different initial dissolved oxygen concentrations. (0, 50, 80, 90 and 100% of saturation). This corresponds to a range of 0–6.53 ppm of

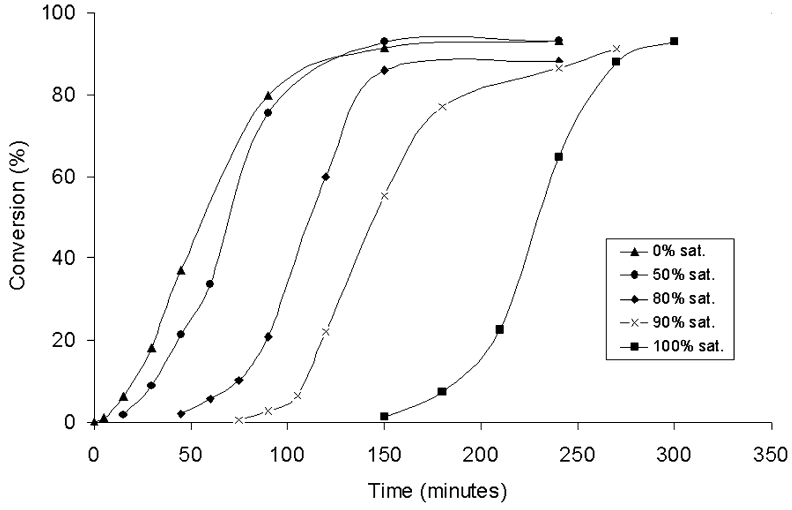

Fig. 1. Conversion versus time profiles for experiments at different initial oxygen levels.

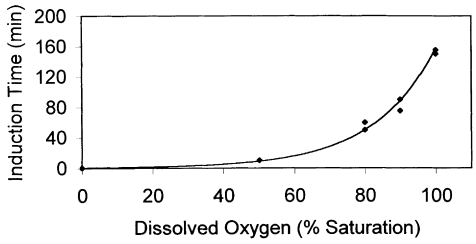

Fig. 2. Induction period for different initial oxygen levels.

oxygen in the aqueous phase. Conversion versus time profiles are shown in Fig. 1. As the initial dissolved oxygen level increased, induction time for the reaction increased, as shown in Fig. 2. Induction times were determined by extrapolating conversion–time data to 0% conversion. There is necessarily some uncertainty, since samples were taken every 15 min. A realistic uncertainty in the induction times is about ±8 min (i.e. half the time between samples). Run to run reproducibility was quite good. Induction time did not vary linearly with dissolved oxygen concentration, as might be expected if the O_2 concentrations in each phase (aqueous phase, styrene droplets, polymer particles, headspace) remained in equilibrium. As the initial O_2 concentration increased, the induction time lengthened dramatically, and in fact can be well modeled by an exponential equation. The possible reasons for this behavior will be discussed later.

Once polymerization commenced, the conversion-time behavior was similar for all runs. For runs having an initially higher O_2 concentration, a more gradual approach to a constant rate is observed, suggesting some degree of retardation at low conversions. All runs exhibited a period of approximately constant rate (constant slope on the conversion-time plots) corresponding to Interval II conditions. These rates were similar for all runs, as were the final conversions (as shown in Table 3). The final O_2 concentrations in all runs were <0.05 ppm.

Analysis of molecular weights reveals the effects of initial O_2 concentration on the latex properties (Fig. 3 and Table 4). With a well-purged latex (0% saturation), high molecular polymer is produced from the outset. However as the initial O_2 concentration is increased, lower molecular weight polymer is produced early in the reaction, caused by

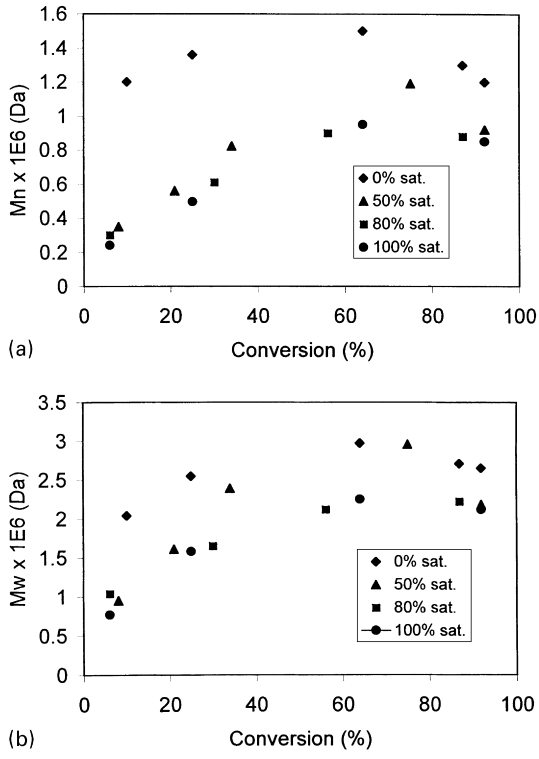

Fig. 3. (a) Number average molecular weight profiles at different initial oxygen levels. (b) Weight average molecular weight profiles at different initial oxygen levels.

premature termination of the growing chains. Higher initial O_2 concentrations result in lower initial molecular weights. However, by the end of the reaction, the molecular weight increased to values similar to those seen in the oxygen-free runs. The final molecular weight averages are not greatly influenced by the presence of oxygen early in the reaction (Table 4).

Mean particle diameter decreases as the initial O_2 concentration increases, as shown in Table 4. This phenomenon, as predicted and observed by Huo et al. [7], is caused by a prolonged nucleation period in the presence of oxygen, resulting in a higher particle number and therefore smaller final particle diameter. With a higher particle number, a higher polymerization rate in Interval II would be expected in the absence of any retardation. In all runs, the mean number of radicals per particle during Interval II was

Table 3
Summary of average reaction rates during interval II and final conversions for different oxygen saturation levels

Dissolved oxygen level (% saturation)	Rate for interval II ($\times 10^{-4}$ mol/s/dm^3)	Final conversion (%)
0	7.50	92, 91, 93
50	8.25	94
80	7.35	98, 88
90	7.50	98, 90
100	6.75	90, 95

Table 4
Summary of final average molecular weight data and final particle size

Dissolved oxygen level (% saturation)	M_n ($\times 10^{-6}$)	M_w ($\times 10^{-6}$)	Mean final particle diameter (μm)
0	1.23, 1.16, 0.983	2.65, 2.45, 2.05	102 ± 5
50	0.920	2.18	89 ± 5
80	0.883, 0.851	2.22, 2.07	80 ± 5
90	0.845, 0.902	2.11, 2.38	77 ± 5
100	0.851, 0.908	2.12, 2.39	68 ± 5

Table 5
Moles of dissolved oxygen in each phase at different initial oxygen levels

Dissolved oxygen level (% saturation)	Aqueous phase ($\times 10^{-5}$ mol)	Styrene phase ($\times 10^{-4}$ mol)	Headspace ($\times 10^{-4}$ mol)	Total ($\times 10^{-3}$ mol)
50	5.56	1.12	8.42	1.01
80	8.90	1.79	13.5	1.61
90	10.0	2.01	15.2	1.82
100	11.1	2.23	16.8	2.02

~0.5 (range varied from 0.47 to 0.50). Most styrene emulsion polymerizations follow zero-one kinetics, although pseudobulk kinetics can occur under some conditions. Rate is proportional to particle number for zero-one kinetics, but becomes independent of particle number in the pseudobulk regime. From the available gravimetric data, it is not possible to make conclusive statements about comparative reaction rates, other than to say they are approximately the same during Interval II for all runs, and that zero-one kinetics during Interval II are followed in all runs.

4. Discussion

It has been recognized previously that increased induction periods result from increased oxygen levels, but quantitative assessments of how induction periods vary with O_2 concentration have not been previously reported. Before attempting to interpret the observed induction period data, a discussion of the distribution of oxygen within the different phases of reactor is warranted. Prior to the start of reaction, dissolved oxygen will be present in the aqueous phase, styrene monomer droplets, micelles (which are swollen with monomer) and the reactor headspace. Oxygen has traditionally been considered to be a "water-soluble" inhibitor, but it is more appropriately treated as being both monomer-soluble and water-soluble [1,7]. Because the source of radicals in emulsion polymerization is the aqueous phase, it is there where most radicals are consumed. Oxygen is believed to diffuse from the styrene droplets and particles into the aqueous phase and thus serves to replenish the oxygen being consumed by reactions with aqueous phase radicals [7]. The potential role of headspace oxygen has also been discussed by de Arbina et al. [1] and Nomura et al. [9]. Prolonged retardation effects were attributed to a continuous diffusion of oxygen from the reactor headspace to the latex. Oxygen diffusion from droplets, particles, or micelles to the aqueous phase and from the headspace to the aqueous phase must both be considered in interpreting data.

Assuming there is equilibrium between all phases at the beginning of reaction, consumption of oxygen in the aqueous phase by reaction with radicals will reduce the oxygen concentration in the aqueous phase and thus provide the driving force for diffusion from the other phases. It is likely that oxygen diffusion from either droplets, particles or micelles into the aqueous phase will be relatively fast, given the high interfacial areas and the comparable solubility of oxygen in water and styrene. (Oxygen is in fact more soluble in styrene than water. Little data is available, but extrapolation of data from 15–35°C [16] suggests the solubility of oxygen in styrene at 60°C is about 35 ppm, compared to 5.4 ppm in water. This estimate of oxygen solubility is considerably lower than the value reported by Miller and Mayo [17] based on unpublished data but is considered more reliable.) Diffusion of oxygen from the headspace to the aqueous phase of the latex will likely be considerably slower, primarily due to the very low interfacial area. If we assume all styrene is present in 20 μm diameter droplets, the ratio of the styrene–water interfacial area to the gas–liquid interfacial area is $\sim 10^{11}$ in a 1 l reactor. (It will be even greater in large reactors.) It is therefore reasonable to assume that equilibrium O_2 concentrations will be maintained between the organic and aqueous phases, but not between the gas and liquid phases.

The moles of oxygen present in each phase for each of the saturation conditions used in this study are shown in Table 5. The values for the aqueous phase are based on measured data. Knowing the 100% saturation concentration of oxygen in the styrene, the concentrations of oxygen in styrene at varying saturation levels were calculated by taking the appropriate fraction of the saturation value. (These values assume an oxygen solubility in styrene of 35 ppm [16] and a total pressure of 1 atm.) It was assumed all phases were in equilibrium at the beginning of reaction, which is justified given the long times allowed for the oxygen measurement to stabilize prior to starting the polymerization. The number of moles of headspace oxygen was calculated using the ideal gas law.

Table 5 reveals that most of the oxygen present in the reactor is in the headspace (83%), and comparatively small amounts are present in the aqueous (6%) and organic phases (11%). These calculations show that the headspace is a larger reservoir of oxygen, and justify concerns that previous authors have expressed about the role of gas phase oxygen having prolonged affects on the course of reaction, particularly under conditions such as vigorous agitation where the rate of gas–liquid mass transfer could be high.

Further light is shed on the values shown in Table 5 if we

Table 6
Induction time predicted for each phase assuming all oxygen is consumed by primary radicals from initiator decomposition

Dissolved oxygen level (% saturation)	Aqueous phase predicted induction time (min)	Styrene phase predicted induction time (min)	Headspace predicted induction time (min)	Observed induction time (min)
50	44	87	659	10
80	70	140	1054	55
90	78	157	1186	80
100	87	175	1318	150

consider how long an induction period would result due to the oxygen in each phase. This calculation requires the initiator concentration and the decomposition rate parameter, k_d [18]. Table 6 shows the predicted induction time corresponding to complete consumption of all oxygen in each phase by decomposing initiator. A comparison of theoretical induction times with those obtained experimentally reveals that the actual induction periods are all much shorter than would be expected if all the oxygen was consumed. In fact the induction times indicate even some aqueous and styrene phase oxygen is still present when polymerization commences. This further suggests that some retardation should be observed, since polymerization is commencing with some oxygen still present in the liquid phases. As will be seen, the molecular weight data support this supposition. Only a small portion of the headspace oxygen is probably consumed. If the headspace oxygen did diffuse into the latex at an appreciable rate, the observed induction periods would have been considerably longer.

The exponential dependence of induction time on initial O_2 concentration provides evidence for slow diffusion of oxygen from the reactor headspace into the latex. If there were no diffusion from the headspace, a linear relationship would be observed between the initial O_2 concentration and induction time. However it appears that prolonged mixing periods do allow sufficient oxygen to diffuse into the latex from the headspace to prolong the induction period. For runs with lower initial O_2 concentration, oxygen will still diffuse from the headspace but the effects will not be as apparent or easy to observe once the polymerization commences.

Molecular weight data as a function of conversion (Fig. 3) provide further evidence that retardation effects are present in addition to inhibition. As the initial O_2 concentration increases, the initial molecular weight is considerably reduced compared to the initial molecular weight with a well-purged system. While an induction period is clear evidence of oxygen inhibiting the aqueous phase kinetics, the presence of low molecular weight polymer is a clear indicator that oxygen remains in the organic phase at the start of the polymerization. As the reaction progresses, the organic phase oxygen will also be consumed, causing the molecular weight to increase to the value observed in the absence of oxygen. This initial retardation is also evidenced by the gradual increase in reaction rates observed in the conversion–time plots (Fig. 1). These observations are consistent with the previous calculations showing that some oxygen probably remains in the organic phase at the start of polymerization.

Particle diameter decreases as the initial O_2 concentration in the latex increases. This observation is consistent with the findings and predictions of Huo et al. [7]. This effect is more pronounced with monomer-soluble inhibitors, which can retard the particle growth rate early in the reaction, thereby prolonging the nucleation period and resulting in a greater number of particles. Given the higher particle number, a higher polymerization rate would be expected for runs with higher initial O_2 concentration. A higher reaction rate may occur once all the oxygen still present in the organic phase at the start of polymerization is consumed, but retardation early in the reaction will lower the rate. These competing effects will partially offset each other, which may explain why the observed conversion-time data in our experiments do not show significant rate differences between the different conditions.

High O_2 concentrations in the aqueous phase effectively inhibit nucleation of particles, inferring that ~100% of radicals arising from initiator decomposition are terminated. As the oxygen is consumed, it will at some time reach a sufficiently low concentration that a small portion of primary radicals will survive long enough to add two or three monomer units in the aqueous phase. If this occurs, the aqueous radicals will have enough surface activity to nucleate micelles and thus initiate polymerization.

Gilbert [19] has developed an expression for initiator efficiency 'f' in emulsion polymerization:

$$f = \left(1 + \frac{\sqrt{k_{t,aq} k_d [I]}}{k_{p,aq} C_w}\right)^{1-z} \quad (1)$$

where $k_{t,aq}$ is the aqueous termination rate parameter, $k_{p,aq}$ is the aqueous propagation rate parameter, C_w is the aqueous phase monomer concentration, and [I] is initiator concentration. The efficiency is determined by the relative probability of a aqueous oligomeric radical surviving long enough to add the critical number of monomer units 'z' required for entry into a micelle or particle versus the probability of it terminating in the aqueous phase prior to reaching the critical length for entry. Gilbert's expression can be modified to account for oxygen inhibition. Extending

Table 7
Parameters used to calculate initiator efficiency 'f'

Parameter	Value	Reference
$k_{p,aq}$	356 dm^3/mol/s	[19]
$k_{t,aq}$	4×10^9 dm^3/mol/s	[19]
k_z/k_p	14,600	[21]
k_d	8×10^{15} (s^{-1}) exp[-135(kJ/mol^{-1})/RT]	[18]
C_w	5.02×10^{-3} mol/dm^3	[20]

the original development [19] to account for the added inhibition step, the modified expression for the initiator efficiency becomes:

$$f = \left(1 + \frac{\sqrt{\left(k_{z,aq}[O_2]\right)^2 + 16k_{t,aq}k_d[I]}}{4k_{p,aq}C_w}\right)^{1-z} \quad (2)$$

where $k_{z,aq}$ is the aqueous inhibition rate parameter and $[O_2]$ is the aqueous phase oxygen concentration. Using this expression, quantitative predictions of initiator efficiency as a function of O_2 concentration can be made. These calculations provide most insight near the end of the inhibition period when there will still be a finite, non-zero O_2 concentration in the water, and yet polymerization may commence nonetheless.

The initiator efficiency can be evaluated if the following parameters are known: $k_{p,aq}$; $k_{t,aq}$; C_w; k_d; $k_{z,aq}$ and the critical length for entry 'z'. The values for $k_{p,aq}$, $k_{t,aq}$, C_w, and k_d can be taken from the literature. A value of 2.0 has been used for 'z'. Table 7 summarizes the parameter values used. The inhibition constant $k_{z,aq}$ can be approximated from the k_z in styrene [21] if it is assumed that the ratio k_z/k_p is the same for oligomeric radicals in water as it is for macroradicals in styrene. (The rationale of assuming the equivalence of k_p and $k_{p,aq}$, has been established [19]). For styrene emulsion polymerizations 'f' is typically quite low, even in the absence of oxygen (~10% or less) [19]. Fig. 4 shows how the initiator efficiency varies with $[O_2]_{aq}$ as calculated using Eq. (2). Curves are shown for all the initial oxygen levels used. The very high value of the inhibition constant ensures that 'f' is close to zero at moderate-high values of $[O_2]_{aq}$. At lower values of $[O_2]_{aq}$, however, 'f' increases rapidly and approaches the value found in the absence of oxygen (0.16 for the experimental conditions used in this work). As the oxygen is consumed, an increasing fraction of the aqueous radicals will be able to enter particles. While the efficiency may still be lower than in the absence of oxygen, the entry rate can still be sufficiently high to initiate polymerization. When this happens, the initial phase of the conversion-time curve will resemble that of a run with much lower [I] than is actually present. The nucleation period will be prolonged and thus the approach to a constant (or near constant) rate in Interval II will be slowed. Data from Figs. 2 and 4 taken together suggest that 'f' is ~0.02 when polymerization commences, regardless of the initial oxygen level.

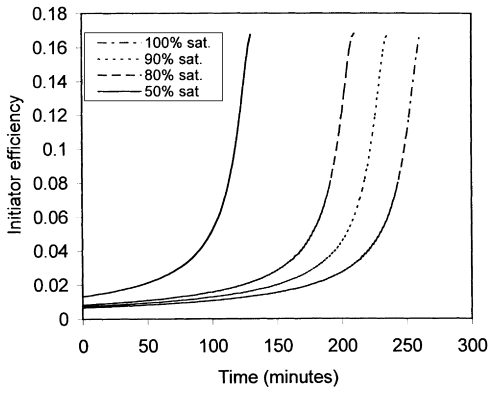

Fig. 4. Calculated initiator efficiency 'f' for different initial oxygen levels. Parameters used in calculation are shown in Table 7. Critical entry length of oligomer (z) = 2.

The induction time data our experiments can be used with the known value of k_d and [I] to crudely estimate $[O_2]_{aq}$ at the start of polymerization. The initial value of $[O_2]_{aq}$ was measured, and the production rate of radicals from initiator decomposition can be calculated ($2k_d$[I]). If the cumulative moles of primary radicals generated from the beginning of reaction to the end of the induction period are subtracted from the initial moles of *both* aqueous and organic phase oxygen (recall we are assuming they are in equilibrium), the total moles of remaining oxygen in both the aqueous and styrene phases (at the end of the induction period) is obtained. Relative solubilities of oxygen in each phase are then used to estimate $[O_2]_{aq}$ at the end of the induction period, assuming negligible oxygen enters from the headspace. The results of theses calculation for the conditions used in this study are shown in Table 8. For all runs, the calculated values of $[O_2]_{aq}$ at the end of the induction period range from ~3–4 ppm. The approximate constancy of these values is curious, and suggests that for the primary radical generation rate used in our experiments, the initiator efficiency reached a sufficiently high value to initiate polymerization at ~3 ppm oxygen. This estimation assumes equilibrium between the liquid phases. If oxygen diffusion from the droplets and particles was slow, the actual $[O_2]_{aq}$ would be lower. This observation suggests an interesting paradox, that the induction period should approach 0 min at ~50% saturation. This is not quite

Table 8
Calculated oxygen levels in aqueous phase (ppm) at end of induction period

Dissolved oxygen (% saturation)	Calculated oxygen level at end of induction period (ppm)	Initial oxygen level (ppm)
50	3.0	3.27
80	3.7	5.22
90	3.8	5.88
100	2.9	6.53

what is experimentally observed (Fig. 2), but it does suggest that low oxygen levels may in fact yield no induction periods, provided the primary radical generation rate is sufficient.

A low but non-zero oxygen concentration in the aqueous phase also implies the presence of oxygen in particles and droplets (assuming water–styrene equilibrium is maintained). If this was true, we would expect to see evidence of retardation near the beginning of polymerization. In fact both the conversion-time data and the molecular weight data show that retardation does exist at low conversions, verifying the qualitative correctness of these calculations.

5. Conclusions

Measurements of initial aqueous phase dissolved oxygen levels in styrene emulsion polymerization show that oxygen is most appropriately treated as both a water-soluble and monomer-soluble inhibitor. Induction periods increase nonlinearly with initial oxygen levels, suggesting diffusion of oxygen from the headspace to the latex can have a significant impact on reaction rates and polymer properties. Partitioning calculations showed that the headspace could be a large source of oxygen, much greater than either the aqueous or styrene phases. At higher initial oxygen levels, low molecular weight polymer was produced early in the polymerization, signifying retardation in the particle phase. As the oxygen was consumed during reaction, the molecular weight gradually increased. Higher initial oxygen levels also resulted in lower mean particle diameter due to a prolonged nucleation period.

Acknowledgements

The financial support of the Natural Sciences and Engineering Research Council of Canada is gratefully acknowledged.

References

[1] de Arbina LL, Gugliotta LM, Barandiaran MJ, Asua JM. Polymer 1998;39:4047–55.
[2] McKenna TF, Graillat C, Guillot J. Polym Bull 1995;34:361–8.
[3] Saenz JM, Asua JM. J Polym Sci A 1995;33:1511–21.
[4] Paul Ch, Schmidt-Naake G. DECHEMA Monographs 1995;31:271–9.
[5] Hattori M, Sudol ED, El-Aasser MS. J Appl Polym Sci 1993;50:2027–34.
[6] Penlidis A, MacGregor JF, Hamielec AE. J Appl Polym Sci 1988;35:2023–38.
[7] Huo BP, Campbell JD, Penlidis A, MacGregor JF, Hamielec AE. J Appl Polym Sci 1987;35:2009–21.
[8] Hasan SM. J Polym Sci A 1982;20:2969–78.
[9] Nomura M, Harada M, Eguchi W, Nagata S. J Appl Polym Sci 1972;16:835–47.
[10] Mork PC. Eur Polym J 1969;5:261–71.
[11] Dunn AS, Taylor PA. Makromol Chem 1965;83:207–19.
[12] Bovey FA, Kolthoff IM. J Am Chem Soc 1947;69:2143–53.
[13] Kolthoff IM, Dale WJ. J Am Chem Soc 1947;69:441–6.
[14] Price CC, Adams CE. J Am Chem Soc 1945;67:1674–80.
[15] Perry RH, Green DW, editors. Perry's chemical engineers' handbook 7. New York: McGraw Hill, 1997.
[16] Encyclopedia of polymer science and engineering, 1989, New York: Wiley.
[17] Miller AA, Mayo FR. J Am Chem Soc 1956;78:1017–23.
[18] Behrman EJ, Edwards JO. Rev Inorg Chem 1980;2:179–206.
[19] Gilbert RG. Emulsion polymerization: a mechanistic approach, London: Academic Press, 1995.
[20] Lane WH. Ind Eng Chem (Anal Chem) 1946;18:295–6.
[21] Henrici-Olive G, Olive S. Makromol Chem 1957;24:64–75.